# Ventral tegmental area dopamine controls timing variability

Matthew A. Weber[1], Kartik Sivakumar[2], Alexandra S. Bova[1], Ervina E. Tabakovic[1], Mackenzie M. Conlon[1], Mayu Oya[3], Rachel C. Cole[4], Arturo I. Espinoza[5], Youngcho Kim[1], Nandakumar S. Narayanan[1]

[1] Department of Neurology, Carver College of Medicine, University of Iowa, Iowa City, IA 52242,
[2] West Virginia University Medical Science Training Program, P.O. Box 9024 Morgantown, WV 26506
[3] Johns Hopkins University School of Nursing, Baltimore, MD 21205
[4] University of Minnesota, Minneapolis, MN 55455
[5] Des Moines University, Des Moines, IA 50312

***Corresponding Author**
Nandakumar Narayanan
nandakumar-narayanan@uiowa.edu

**ABSTRACT**

Precision defines successful behavior, yet the brain mechanisms promoting precision are unclear. Here, we dissect dopaminergic circuits controlling precision along a single behavioral dimension – the timing of action. We use an interval timing paradigm that requires participants to indicate their estimate of an interval of several seconds with a motor response. We find that humans with Parkinson's disease (PD) had increased timing variability that predicted PD-related cognitive deficits and executive dysfunction. Surprisingly, lesioning ventral tegmental area (VTA) dopamine neurons increased temporal variability. Further, GCaMP6s fiber photometry demonstrated that VTA dopamine neuron activity is strongly modulated at the start of temporal intervals, and that this trial start-related activity predicted temporal variability. Finally, we found that stimulation of VTA dopamine neurons improved timing by decreasing temporal variability in both intact and dopamine-depleted animals. Our data establish a model of cognitive symptoms of human PD and provide insight into the neuronal control of temporal variability, which impacts a wide range of executive functions.

## INTRODUCTION

To be effective, behavior must be accurate as well as precise. While much of behavioral neuroscience has focused on accurate behavioral outcomes, considerably less effort has been focused on behavioral precision and variability[1,2]. A neurotransmitter system that is critical for behavioral variability is dopamine, as drugs and diseases of dopamine can modulate behavioral variability[3–5]. However, it is unclear how dopamine modulates precise behavior, which is important to understanding a wide range of mammalian behavior as well developing new biomarkers and treatments for human diseases such as schizophrenia, attention-deficit hyperactivity disorders, substance use disorder, and Parkinson's disease (PD)[6–8].

Complexity can challenge attempts to quantify behavioral variability. We addressed this by turning to a paradigm configured to capture behavioral variability – interval timing[9]. This paradigm requires participants to estimate an interval of several second by making a motor response and measures temporal precision by quantifying the variability of responses[10]. Past work has shown that humans with disrupted dopamine, including schizophrenia and Parkinson's disease, have increasing timing variability[11–16], which implicates dopaminergic circuits in temporal variability.

We systematically investigated dopaminergic circuits and temporal variability. We found that PD patients had increased timing variability that predicted executive dysfunction and cognitive status. In mice, we found that depleting dopamine in the ventral tegmental area increased timing variability and that ventral tegmental area dopaminergic neuron activity triggered at the start of timing trials predicted timing variability. Further, we found that stimulating ventral tegmental dopamine neurons improved timing by decreasing timing

variability in intact and dopamine-depleted animals. We interpret our data in the context of ventral tegmental dopamine and cognitive variability.

## METHODS

*Humans:* We recruited 94 Parkinson's disease (PD) patients and 43 health comparison control participants from the movement-disorders clinic at the University of Iowa according to methods described in detail previously[12,17]. Patients were examined by a movement-disorders physician to verify that they met the diagnostic criteria recommended by the United Kingdom PD Society Brain Bank. We obtained written informed consent from each participant (IRB Protocol 201707828). PD patients participated in the study while taking their prescribed medications, including levodopa, as usual. All testing was done in a laboratory setting in the University of Iowa's Department of Neurology. All stimuli were presented via Psychtoolbox v3.0, a MATLAB toolbox running on a Dell XPS workstation and MATLAB 2018b, and a 19-inch monitor. We performed a peak interval timing task with 3-second and 7-second trials randomly intermixed[17] that required participants to estimate a duration of either 3 seconds or 7 seconds after reading instructions displayed as text at the center of a video screen. White instructional text on the center of a black screen was presented that read "Short interval" on 3-second interval trials and "Long interval" on 7-second interval trials. Interval durations were never communicated to the patient. After the instructions were displayed for 1 second, the start of the interval was indicated by an imperative "Go" cue: an image of a solid box in the center of the computer screen. The cue was displayed on the screen for the entire trial, which lasted 8–10 s for 3-second intervals and 18–20 s for 7-second intervals. Participants were instructed to estimate the duration of the intervals without counting. As a distraction to discourage counting, vowels appeared at random intervals in the center of the screen. Participants were instructed to press the keyboard spacebar at the start of when they judged the target interval to have elapsed. On 15% of the trials, participants were then given nonnumerical/nonverbal performance feedback on the screen

98 indicating their response relative to the actual target interval; feedback was a horizontal green
99 line indicating how close their keypress was to the target time. Because feedback was relatively
100 infrequent, we did not analyze this event. The time between trials varied from 3–8 seconds. All
101 participants performed 6 training trials prior to testing trials and verbalized understanding of the
102 task. Testing sets consisted of 40 trials of each interval length, for a total of 80 trials. Trials were
103 presented in a random order of 20 trials blocks; four blocks were presented. Participants took a
104 self-paced break between each block and moved to the next block by pressing any key. We
105 analyzed the mean keypress time to capture timing accuracy for PD patients and control
106 participants. To analyze timing precision, we computed the coefficient of variance (CV) by
107 dividing the standard deviation by the mean keypress time. Of note, data from some participants
108 was included in prior work[12,17].

109

110 *Mice:* All experimental procedures were approved by the Institutional Animal Care and Use
111 Committee (IACUC) at the University of Iowa and performed in accordance with relevant
112 guidelines of Protocol #3052039. Two different strains of mice were used: 1) wild type male and
113 female C57BL/6 mice received from Jackson Labs (Bar Harbor, ME) at approximately 12–14
114 weeks of age; and 2) heterozygous male and female $DAT^{IRES}$-Cre
115 (B6.SJL-Slc6a3tm1.1(cre)Bkmn/J) mice bred in house from breeding pairs received from
116 Jackson Labs (Strain #:006660). Prior to behavioral training or surgical procedures, all mice
117 were communally housed on a 12-hour light/dark cycle with *ad libitum* access to laboratory
118 rodent chow and water. To facilitate operant behavioral training, mice were individually housed
119 and maintained on a restricted diet with *ad libitum* access to water.

120

121 *Interval timing switch task:* We used a mouse optimized interval timing task described in depth
122 previously[18–25]. Mice were trained in standard sound attenuated operant chambers
123 (MedAssociates, St. Albans, VT) with a reward hopper located between the two nosepoke
124 response ports (left and right) on the front wall and another nosepoke on the back wall. Each
125 90-minute session was randomly organized into 50% "short" 6 second interval trials and 50%
126 "long" 18 second interval trials. Short and long trials had identical audio and visual cues and are
127 self-initiated by a response at the back nosepoke port. In a short trial, mice must respond as the
128 designated nosepoke after 6 seconds to then receive a 20 mg sucrose reward (BioServ,
129 Flemington, NJ). This short designated nosepoke is counterbalanced left vs. right across mice.
130 When a short trial is initiated, mice begin by responding at the designated nosepoke; mice may
131 respond multiple times, but the reward is only delivered for the first response after 6 seconds. In
132 a long trial, mice must respond at the opposite nosepoke, which is designated for long trials in
133 which mice receive a reward for the first response after 18 seconds. Since cues are identical for
134 both short and long trials, the optimal strategy is for mice to start responding at the designated
135 short trial nosepoke, but if enough time passes with no reward delivered, the mice switch to the
136 designated long trial nosepoke. The switch response time is defined as the moment when the
137 mouse leaves the short trial nosepoke and is a measure of the rodent's internal estimate of time,
138 as in other interval timing tasks[19,21]. Only the long trials in which mice make an appropriate
139 switch are analyzed[18–20,22–25].

140

141 *Surgical procedures*: Surgical methods were identical to those described previously[19,22,25,26].
142 Mice were anesthetized with 4.0% isoflurane at 400 mL/min and maintained on 1.5%–3.0%
143 isoflurane at 120 mL/min (SomnoSuite, Kent Scientific, Torrington, CT, USA). Craniotomies

144 were drilled above the ventral tegmental area (AP +3.3 mm / ML ±1.1 mm). Viruses,
145 neurotoxins, or vehicles were infused over 10 minutes (0.05 μL/min; Legato 130 Syringe Pump,
146 kd Scientific, Holliston, MA), with a 5-minute wait period before removing the needle. For fiber
147 photometry and optogenetic experiments, at least three stainless steel screws were attached to the
148 skull to stabilize head cap assemblies, which were sealed with cyanoacrylate ("SloZap," Pacer
149 Technologies, Rancho Cucamonga, CA) and accelerated with "ZipKicker" (Pacer Technologies)
150 and methyl methacrylate (AM Systems, Port Angeles, WA). Following all surgical procedures,
151 mice were allowed at least 1 week to recover before starting food restriction and interval timing
152 training.

153 For dopamine depletion experiments[22], wild type C57BL/6J mice were first trained on the
154 interval timing switch task described above for approximately 3–4 weeks before surgical
155 procedures. On the day of surgery, 6 hydroxydopamine hydrobromide (6-OHDA; Millipore
156 Sigma #162957, Darmstadt, Germany) and desipramine hydrochloride (Millipore Sigma
157 #D3900) were freshly made and stored on ice away from light. 6-OHDA was prepared at 2
158 mg/ml in 0.03% ascorbic acid (AA) and desipramine at 4 mg/ml in 0.9% saline. Desipramine (25
159 mg/kg) was injected intraperitoneally (IP) prior to starting surgical procedures to protect
160 norepinephrine terminals against 6-OHDA[27–29]. Mice were randomly assigned to either the
161 vehicle group or the ventral tegmental area dopamine depletion group. The vehicle group
162 received microinjections of 0.5 μl 0.03% AA bilaterally, and the dopamine depletion groups
163 received equal volumes of 6-OHDA prepared in AA (DV -4.6 mm at 10° laterally).

164 For fiber photometry experiments, a Cre-dependent GCaMP6s virus (Addgene,
165 Watertown, MA; Catalog #100845-AAV5; pAAV.Syn.Flex.GCaMP6s.WPRE.SV40) was
166 unilaterally injected in the VTA (DV -4.6 mm at 10° laterally) of $DAT^{IRES}$-Cre mice. A fiber

167 optic cannula (Doric Lenses Inc, Quebec, Cananda; NA 0.48) was then implanted in the VTA
168 (DV -4.5 mm at 10° laterally).

169 For optogenetic stimulation experiments, a Cre-dependent channelrhodopsin[30] (ChR2;
170 Addgene; Catalog #20297-AAV5; pAAV-EF1a-DIO-hChR2(H134R)-mCherry) was bilaterally
171 injected in the VTA (DV-4.6 mm at 10° laterally) followed by implantation of bilateral fiber
172 optics (Doric Lenses Inc; NA 0.22; DV -4.5 mm at 10° laterally). There were two separate
173 cohorts of optogenetic stimulation mice. In one cohort, only Cre-dependent ChR2 was injected in
174 the VTA. In the other cohort, 6-OHDA was injected first using the same procedures as the
175 dopamine depletion experiments described above; desipramine was also injected to preserve
176 norepinephrine terminals. After 6-OHDA VTA injections, Cre-dependent ChR2 was injected and
177 fiber optics implanted as described above.

178

179 *Fiber Photometry:* Mice were extensively trained in the interval timing task described above
180 before being acclimatized to fiber photometry procedures. Mice were unilaterally tethered to an
181 optical patchcord connected to a fiber photometry system (Doric Lenses, Inc; Québec, Cananda)
182 with two excitation wavelengths (405-nm LED isosbestic signal modulation at 208.616 Hz and
183 470-nm LED $Ca^{2+}$-dependent GCaMP6s signal modulated at 572.205 Hz). Isosbestic and
184 GCaMP6s fluorescence wavelengths were measured via integrated LED mini cubes and
185 photodetector (iLFMC4, Doric Lenses, Inc). Changes in GCaMP6s fluorescence were
186 downsampled to 100 Hz, low-pass filtered at 5 Hz, detrended to compensate for exponential
187 decay and photobleaching, motion corrected and normalized via the fitted isosbestic signal to
188 calculate $\Delta F/F_0$, z scored across the entire session, and aligned to task events[26,31].

189

190 *Optogenetics*: Similar to fiber photometry recordings, mice were extensively trained prior to
191 optogenetic stimulation procedures. Mice were tethered to a 473-nm laser diode (Doric Lenses,
192 Inc) through a bilateral optical rotary joint and optical patchcords (both from Doric Lenses,
193 Inc)[19,32]. Laser power output was adjusted prior to each session to 12 mW at the tips of the
194 optical patch cords. Optogenetic stimulation was controlled with custom written Arduino
195 protocols and delivered during the first 2 seconds of randomly selected trials controlled by
196 MedAssociates. Separate sessions were run with laser stimulation delivered at either 4 Hz or 20
197 Hz. We focused on interval timing switch trials and compared mean switch response time and
198 switch response time CV when no laser light was delivered vs. when laser light was delivered.

199

200 *Histology*: Mice were sacrificed following the completion of all experiments. Mice were deeply
201 anesthetized using ketamine (100 mg/kg IP) and xylazine (10 mg/kg IP) and transcardially
202 perfused with phosphate buffered saline (PBS) and 4% paraformaldehyde (PFA). Brains were
203 removed and fixed in 4% PFA overnight, followed by immersion in 30% sucrose for
204 approximately 48 hours, and then frozen in cryoprotectant at -80 ºC. Brains were sliced at 40 µm
205 coronal sections of the midbrain using a cryostat (Leica Biosystems, Deer Park, IL). Selected
206 sections were then stained to visualize tyrosine hydroxylase, according to methods described
207 previously[20,23], as well as native fluorescence of GCaMP6s[26] or ChR2[33,34]. All images were
208 captured using VS ASW S6 imaging software (Olympus, Center Vallet, PA) to confirm
209 histological locations of 6-OHDA dopamine depletion, GCaMP6s and ChR2 fluorescence, and
210 fiber optic locations.

*Statistics*: All data were analyzed with custom code written in MATLAB; all code and data will be available upon final publication at: http://narayanan.lab.uiowa.edu/article/datasets. The two primary measures of interval timing were quantified by 1) the mean switch response time of all switch trials performed during an interval timing session and 2) the switch response time coefficient of variance (CV) of all switch trials performed during an interval timing session. CV was calculated as the standard deviation divided by the mean and is expressed as a percentage. For VTA dopamine depletion experiment without optogenetic stimulation, post-surgery mean switch times and switch time CV were normalized to each mouse's pre-surgical baseline to account for mouse specific variability in timing behavior. Differences between interval timing performance in either human or mouse data were computed using ANOVA from linear models (*fitglme* and *anova* in MATLAB). We accounted for human participant-specific or animal-specific variances in all analyses and set statistical significance at alpha 0.05. Pearson's partial correlation (*partialcorr* in MATLAB) was used to determine the strength of relationships between human interval timing and both MOCA and Executive Function, controlling for UPDRS scores. Pearson's partial correlation was also used to determine the strength of relationships between GCaMP6s $\Delta F/F_0$ and both mean switch response and switch response CV, controlling for multiple behavioral sessions from each mouse.

## RESULTS

We analyzed interval timing performance in 94 PD patients and 43 demographically-matched control participants in a two-interval timing task with 3- and 7-second intervals (Fig. 1A)[12]. The cumulative distribution of response times for each trial type (dashed lines: 3-second interval; solid lines: 7-second interval) are shown in Fig. 1B. We found that PD patients had greater mean response times in the 3-second interval timing task (Control: 3.61 ± 0.18 seconds vs. PD: 4.61 ± 0.23 seconds, $p = 0.005$; Fig. 1C) but not in the 7-second interval timing task (Control: 6.15 ± 0.15 seconds vs. PD: 6.41 ± 0.15 seconds, $p = 0.267$; Fig. 1C). However, PD patients had reliably increased coefficients of variance (CV), calculated from the standard deviation over trials divided by the mean response time, on both interval timing tasks (3 seconds – Control: 35.33% ± 3.50% vs. PD: 52.84% ± 2.85%, $p = 0.0004$; 7 seconds – Control: 14.94% ± 1.04% vs. PD: 23.32% ± 1.50%, $p = 0.0002$; Fig. 1D). CV was significantly correlated with cognitive function as measured by the Montreal Cognitive Assessment (MOCA) for both the 3-second (Pearson's rho = -0.25, $p = 0.017$; Fig. 1E) and 7-second (Pearson's rho = -0.53, $p = 4 \times 10^{-8}$; Fig. 1F) intervals. Furthermore, CV also predicted executive dysfunction as measured by the NIH Toolbox Dimension Change Card Sort/Flanker test for both the 3-second (Pearson's rho = -0.29, $p = 0.006$; Fig. 1G) and 7-second (Pearson's rho = -0.48, $p = 2 \times 10^{-6}$; Fig. 1F) intervals. Taken together, these data demonstrate that human PD patients had increased timing variability.

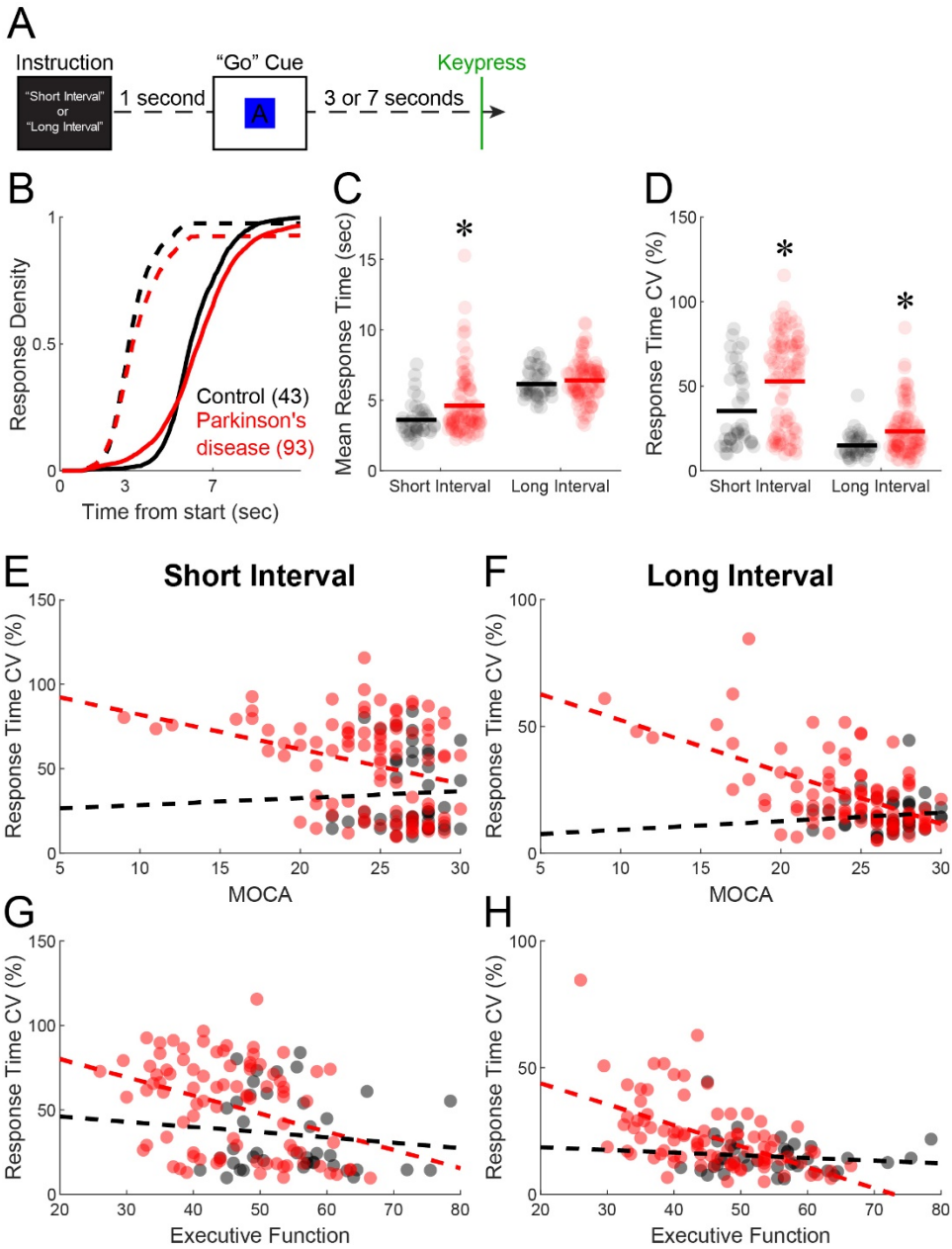


**Figure 1: Human PD patients had increased timing variability. A)** An interval timing task that required participants to press the spacebar when they estimated the target interval to have elapsed. **B)** Cumulative distribution of response times for 3-second (dashed) and 7-second (solid) intervals for control (black) vs. Parkinson's disease (red). **C)** Mean response time and **D)** coefficient of variance (standard deviation/mean) of response times across participants. Response time CV for **E)** 3-second and **F)** 7-second intervals plotted vs. Montreal Cognitive Assessment (MOCA). Response time CV for **G)** 3-second and **H)** 7-second intervals plotted vs. NIH Toolbox Executive Function scores. Data from 94 PD patients and 43 controls. * $p < 0.05$.

We investigated temporal variability using a mouse-optimized interval timing task that requires mice to make a decision to switch between two nosepokes after approximately 6 seconds has passed (Fig. 2A)[18–25,35,36]. We focused on the *switch response time*, defined as the moment mice exit the first nosepoke before responding at the second nosepoke. Switch responses are a time-based decision guided by temporal control of action as no external cue indicates when to switch from one nosepoke to the other.

We examined the effects of VTA dopamine depletion (Fig. 2B) on behavior in the interval timing switch task, which we have previously shown impairs interval timing[37,38]. We normalized post-surgical behavior in the switch task to pre-surgery behavior to determine magnitude change in behavior as a results of VTA dopamine depletion, similar to our previous work[37]. Data from some mice were presented in a previous report[37] but was re-analyzed with additional mice using different methods here. The cumulative distribution of a switch for each mouse is shown in Fig. 2C. In VTA 6-OHDA treated mice, we found no significant change in mean switch time (Vehicle: 104.20% ± 3.68% (relative to presurgical baseline) vs. 6-OHDA: 98.28% ± 5.36%; $p = 0.347$; Fig. 2D), but increased timing variability as measured by the coefficient of variance (CV; Vehicle: 94.66% ± 5.50% vs. 6-OHDA: 135.69% ± 5.36%; $p = 0.001$; Fig. 2E).

There were no changes in trial initiation time (Vehicle: 58.68 ± 6.69 seconds vs. 6-OHDA: 52.38 ± 5.08 seconds; $p = 0.449$), percent of rewarded trials (Vehicle: 67.92% ± 2.26% vs. 6-OHDA: 66.95% ± 3.04%; $p = 0.790$), short responses/trial (Vehicle: 1.55 ± 0.10 vs. 6-OHDA: 1.46 ± 0.07; $p = 0.420$), long responses/trial (Vehicle: 4.50 ± 0.55 vs. 6-OHDA: 3.74 ± 0.25; $p = 0.218$), short response duration (Vehicle: 0.16 ± 0.01 seconds vs. 6-OHDA: 0.17 ± 0.01 seconds; $p = 0.582$), or long response duration (Vehicle: 0.16 ± 0.01 seconds vs. 6-OHDA: 0.17

281 ± 0.01 seconds; $p = 0.367$). Together, these data model deficits in human PD patients and

282 establish a mouse model of cognitive symptoms of PD.

283

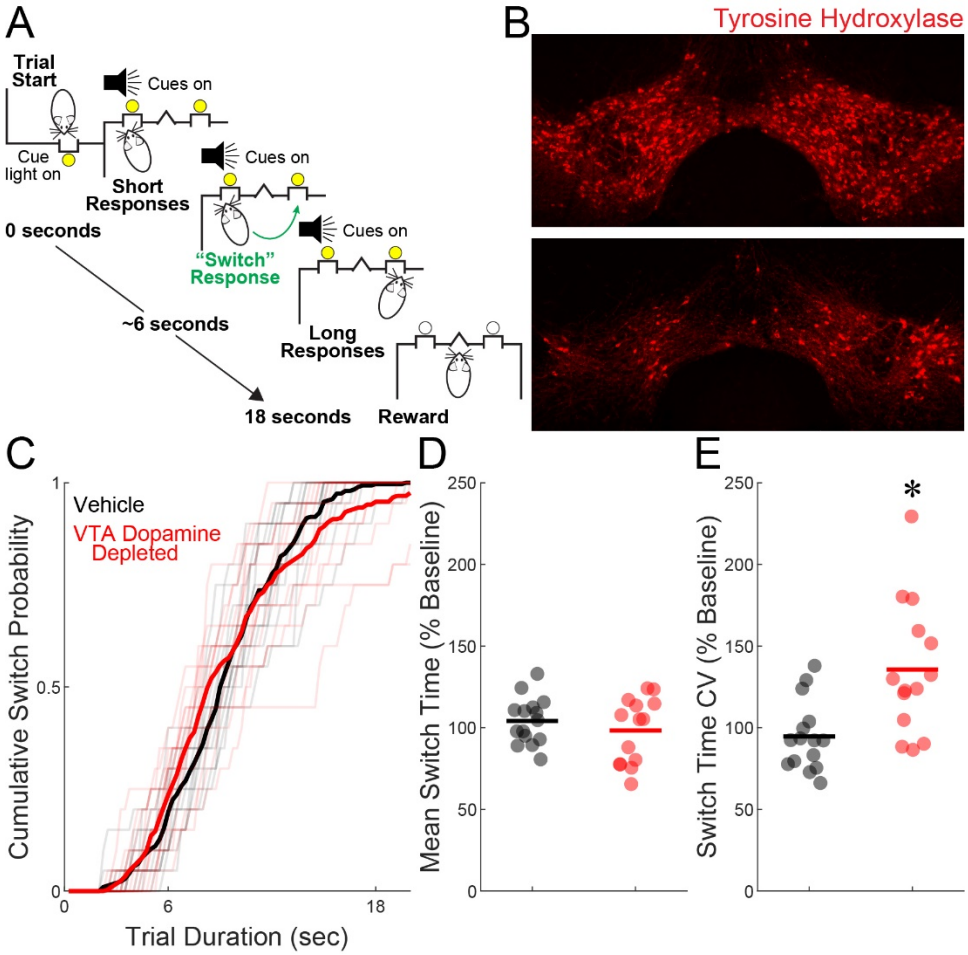


**Figure 2: Ventral tegmental area dopamine depletion increases timing variability. A)** Mouse-optimized interval timing in which trials are initiated at the back nosepoke. Identical cues are delivered for both randomly delivered short and long trials. On short trials, mice are rewarded for the first response after 6 seconds at the designated short nosepoke (left or right). On long trials, mice start by responding at the designated short nosepoke. When there is no reward after 6 seconds, mice switch to the designated long nosepoke (contralateral to designated short nosepoke) and wait until after 18 seconds for reward delivery. This time to switch from the short to long nosepoke is a time-based decision as in other interval timing tasks. Switch time is defined as the time of last response at the short nosepoke before responses start at the long nosepoke, and only switch trials are analyzed. **B)** Representative histological images of TH fluorescence (red) from a mouse injected with ascorbic acid vehicle (top) or 6-hydroxydopamine (6-OHDA; bottom) in the VTA. **C)** Cumulative distribution of switch responses for vehicle (black) and 6-OHDA (red) mice. **D)** Mean switch time and **E)** switch time CV, normalized to behavior prior to the lesion. Data from 15 vehicle and 14 6-OHDA mice. * $p < 0.05$.

Next, we examined the activity of dopamine neurons using the calcium sensor GCamP6s, which was expressed in ventral tegmental dopamine neurons using $DAT^{IRES}$-Cre mice (Fig. 3A-B). During interval timing, we found that VTA dopamine neuron GCaMP6s $\Delta F/F_0$ on average was modulated at trial start, drifted down over the interval, and then increased at trial end in 8 $DAT^{IRES}$-Cre mice. We were interested in which aspects of dopamine neuron activity predicted interval timing behavior, so we analyzed GCaMP6s $\Delta F/F_0$ across 3 sessions from 8 $DAT^{IRES}$-Cre mice. The mean switch time and switch time CV, separated by mouse and session, is shown in Fig 3C-D, respectively. We quantified average changes in VTA dopamine neuron GCaMP6s $\Delta F/F_0$ from both -0.5–0.5 seconds around trial start (Fig. 3E) and from 0.5 seconds to average switch time (Fig. 3F). We found that trial start $\Delta F/F_0$ strongly predicted interval timing variability (Pearson's rho = -0.65, $p$ = 0.001; Fig. 3G) and mean switch time (Pearson's rho = -0.61, $p$ = 0.002; Fig. 3H). We also found that average $\Delta F/F_0$ slope to switch significantly correlated with interval timing variability (Pearson's rho = 0.42, $p$ = 0.045; Fig. 3I) but did not correlate with mean switch time (Pearson's rho = -0.21, $p$ = 0.345; Fig. 3J). These data suggest that VTA dopamine neuron activity is required for and predictive of timing variability.

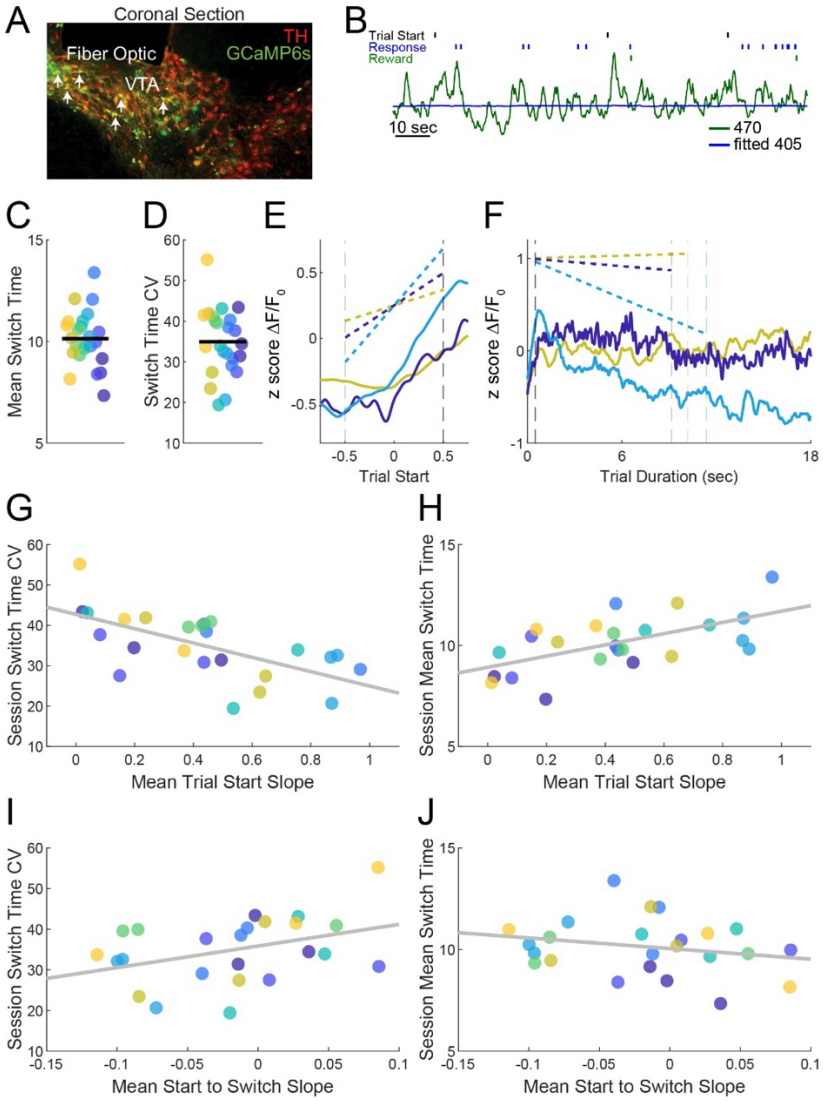


**Figure 4: Ventral tegmental area (VTA) dopamine neuron trial-start activity predicts timing variability. A)** Representative histological images of GCaMP6s fluorescence (green) in the VTA; tyrosine hydroxylase (TH) in red. **B)** Example GCaMP6s (470) and fitted isosbestic (405) trace over 120 seconds of a single interval timing session. **C)** Mean switch time and **D)** switch time CV from GCaMP6s $\Delta F/F_0$ fiber photometry sessions (each color represents a different mouse; 8 $DAT^{IRES}$-Cre mice and 3 sessions per mouse). **E)** $\Delta F/F_0$ trial start slope from 3 different mice with high switch time CV (yellow), moderate switch time CV (dark blue), and low switch time CV (blue). Vertical dashed lines at -0.5 and 0.5 seconds represent the boundaries used to calculate trial start slope. The yellow, dark blue, and blue dashed lines represent the mean slope across all trials for the respective interval timing session. **F)** $\Delta F/F_0$ from trial start to switch from the same sessions as shown in **E**. Vertical dashed lines are at 0.5 seconds and session mean switch time. The yellow, dark blue, and blue dashed lines represent the mean start to switch slope across all trials for the respective interval timing session. **G)** Trial start slope was

330 inversely correlated with CV and **H)** correlated with mean switch time. **I)** There was also a
331 correlation between start-to-switch slope and CV, but **J)** start-to-switch slope did not correlate
332 with mean switch time. Data from 3 sessions in 8 $DAT^{IRES}$-Cre mice. * $p < 0.05$.

333

334 We then tested the hypothesis that stimulating VTA dopamine neurons would decrease
335 timing variability. We expressed channelrhodopsin (ChR2) in the ventral tegmental area of
336 DAT$^{IRES}$-Cre mice. In non-dopamine depleted mice (Fig. 4A), we found that stimulating VTA
337 dopamine neurons at 4-Hz for the 2 seconds, which corresponds to 8 laser pulses, after trial start
338 improved interval timing by decreasing variability (No Stimulation: 36.47% ± 1.17% vs. 4-Hz
339 Stimulation 31.54% ± 1.07%, $p = 0.001$; Fig. 4B-C). There was no change in mean switch time
340 (No Stimulation 9.47 ± 0.22 seconds vs. 4-Hz Stimulation 9.65 ± 0.18 seconds, $p = 0.439$; Fig.
341 4D). Interestingly, 20-Hz stimulation for the same 2 seconds after trial start did not change
342 timing variability (No Stimulation 37.21% ± 1.86% vs. 20-Hz Stimulation 37.70% ± 0.73%, $p =$
343 $0.794$) or mean switch time (No Stimulation 8.74 ± 0.25 seconds vs. 20-Hz Stimulation 8.98 ±
344 0.29 seconds, $p = 0.518$).

345 No effects were observed in control animals with identical stimulation parameters
346 expressing a virus without opsins. There was no change in timing variability at either 4-Hz (No
347 Stimulation 34.03 ± 2.30 vs. 4-Hz Stimulation 34.67 ± 2.33, $p = 0.702$) or 20-Hz (No
348 Stimulation 31.57 ± 2.09 vs. 20 Hz Stimulation 33.77 ± 1.28, $p = 0.287$). There was no change in
349 mean switch time at either 4-Hz (No Stimulation 10.21 ± 0.29 vs. 4-Hz Stimulation 10.29 ± 0.41,
350 $p = 0.760$) or 20-Hz (No Stimulation 9.88 ± 0.11 vs. 20-Hz Stimulation 9.84 ± 0.27, $p = 0.834$).

351 We were interested if VTA dopamine neuron stimulation could compensate for cognitive
352 symptoms of PD. We turned to mice with intermediate dopamine depletion, in which some
353 dopamine neurons remain. Notably, even in human Parkinson's disease, ~30% of dopamine
354 neurons are spared at the end of their disease[39]. Accordingly, we expressed ChR2 in the VTA of
355 DAT$^{IRES}$-Cre mice with dopamine depletion (Fig. 4E). Similar to non-dopamine depleted mice,
356 we found to our surprise that VTA dopamine neuron stimulation at 4-Hz improved interval

timing by decreasing timing variability (No Stimulation 39.72% ± 1.20% vs. 4-Hz Stimulation 35.60% ± 1.41%, $p = 0.003$; Fig. 4F-G) but did not change mean switch time (No Stimulation 10.00 ± 0.26 seconds vs. 4-Hz Stimulation 10.07 ± 0.28 seconds, $p = 0.816$; Fig. 4H). There was no effect of 20-Hz stimulation on timing variability (No Stimulation 41.97% ± 1.64% vs. 20-Hz Stimulation 43.58% ± 1.81%, $p = 0.304$) or mean switch time (No Stimulation 9.43 ± 0.33 seconds vs. 20-Hz Stimulation 9.21 ± 0.30 seconds, $p = 0.486$). Together, these data demonstrate that VTA dopamine neurons control timing variability.

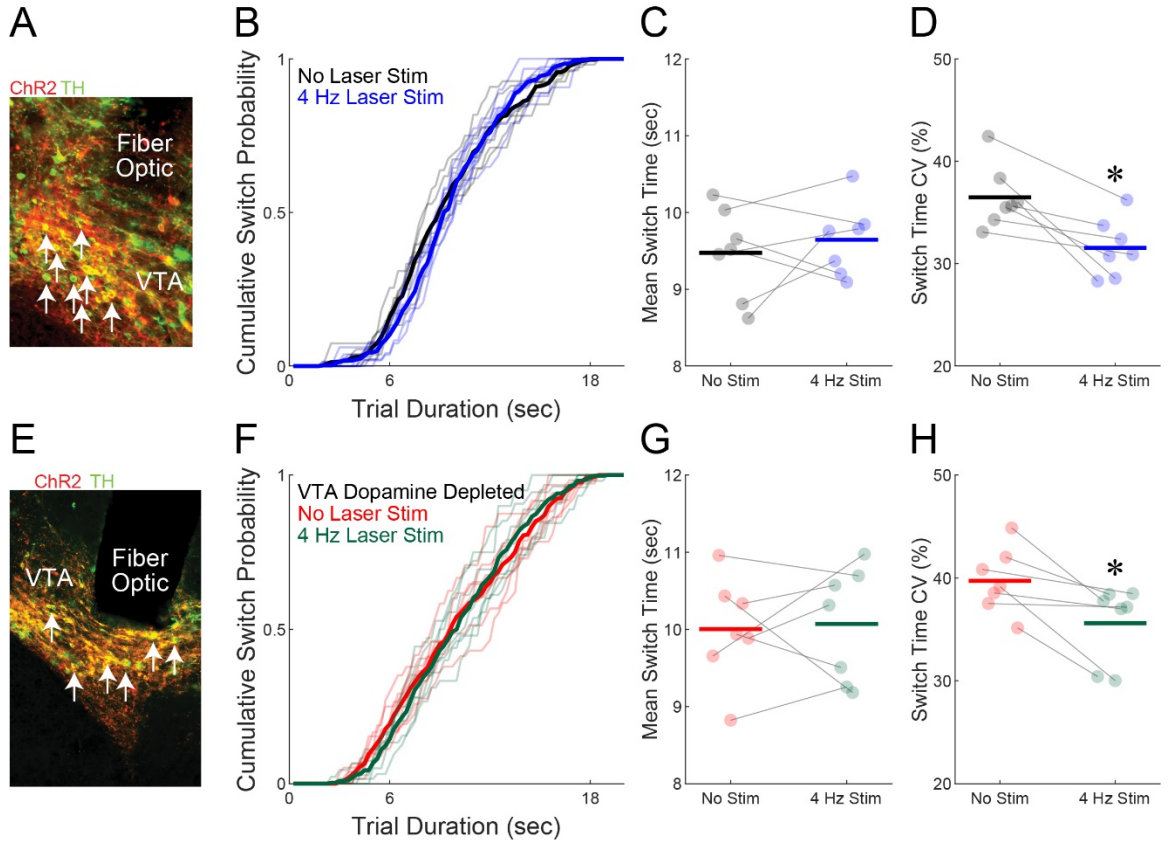


**Figure 5: Stimulating ventral tegmental area (VTA) dopamine neurons improves timing variability. A)** Representative histological images of fiber optics and channelrhodopsin (ChR2; red) in the VTA; tyrosine hydroxylase (TH) in green. **B)** Cumulative switch responses for no stimulation (black) and 4-Hz VTA dopamine neuron stimulation (blue). **C)** There was no change in mean switch time but **D)** there were reliable improvements in timing by decreasing interval timing CV. **E)** In dopamine-depleted mice, representative histological images of fiber optics and ChR2 (red) in the VTA; TH in green. **F)** Cumulative switch responses for no stimulation (red) and 4-Hz VTA dopamine neuron stimulation (green). **G)** There was no change in mean switch time, but **H)** there were reliable improvements in timing by decreasing interval timing CV. Data from 14 $DAT^{IRES}$-Cre mice (7/experiment). * $p < 0.05$.

377 **DISCUSSION**

378 We studied behavioral variability using interval timing. We report three main results.
379 First, PD patients have increased timing variability that predicts cognitive impairment and
380 executive function. Second, we can model this increased timing variability in mice with ventral
381 tegmental area dopamine depletion. Third, VTA dopamine neuron calcium dynamics at the start
382 of temporal intervals is highly predictive of temporal variability across animals. Finally, we find
383 that stimulating VTA dopamine neurons improved interval timing by decreasing temporal
384 variability in intact and dopamine-depleted mice. These data establish that targeting VTA
385 dopamine in mice may model aspects of cognitive dysfunction in human PD[6] and elucidate
386 neuronal circuits controlling behavioral variability.

387 VTA neurons play a key role in motivated behavior. VTA dopamine neurons are
388 heterogenous, projecting to the prefrontal cortex and nucleus accumbens along with other brain
389 stem and subcortical nuclei. Of these, only prefrontal networks are reliably involved in executive
390 dysfunction[40–42]. While much focus has been placed on the role of VTA in motivation and
391 reward[43,44], here we demonstrate a role of VTA dopamine in behavioral variability, independent
392 of reward or motivational effects. Our work is consistent with a role for dopamine in executive
393 function[45]. Indeed, depleting prefrontal dopamine profoundly impairs executive functions such as
394 working memory and interval timing[20,46,47], which requires working memory for temporal rules
395 and attention to the passage of time. Of note, VTA dopaminergic circuits are complex, as VTA
396 dopamine neurons can co-release GABA and glutamate[48,49], and have distinct transcriptional
397 markers such as *Calb1*[50,51]. Future work will need to map this complexity, but the present work is
398 clinically significant because VTA neurons degenerate in PD[39] and may contribute to cognitive
399 symptoms in PD[52].

We found that 4-Hz VTA dopamine neuron stimulation improved interval timing by decreasing variability. This finding is supported by similar work showing that low-frequency prefrontal stimulation of neurons expressing D1-type dopamine receptors improves interval timing[33,34,47] and that 4-Hz cerebellar stimulation improves interval timing in rodent models[53]. In humans, we found that 4-Hz subthalamic nucleus stimulation improved interval timing[54]. Of note, trial start-evoked 4-Hz activity is linked with dopamine, deficits in interval timing, and cognitive symptoms of PD[17,17,33,55,56]. Work by our group and others have found that ~4-Hz deep-brain stimulation of the subthalamic nucleus can improve executive function in PD[54,57–59]. It is unclear how 4-Hz subthalamic nucleus stimulation affects ventral tegmental area or cortical circuits. Importantly, our stimulation was triggered by the start of the interval, while other stimulation paradigms are continuous. Future work will resolve how low-frequency stimulation affects cortical networks, which could be critical to advancing new therapies.

Our work has several limitations. First, we did not explore VTA dopaminergic neuron subtypes or projections[49,50]. Second, we did not explore which cortical or subcortical circuits and neurons are responsible for changing variability, although such effort would require a broad coordinated approach. Finally, we did not deliver brain stimulation to the ventral tegmental area in humans, which would require new surgical planning and dedicated clinical trials. Despite these limitations, our work advances a new role of VTA dopamine neurons in cognitive variability, which is distinct from its traditional role in motivation and reward. Our work will inspire new markers and therapies for human diseases that degrade cognitive variability that may lead to cognitive impairment and dementia.

**Funding:**

This work was funded by NIH R01 NS120987 to NSN.

**Data and Code Availability:**

All code and data will be available upon final publication at: http://narayanan.lab.uiowa.edu/article/datasets.

**Competing Interests:**

The authors declare that there are no conflicts of interest.

**Author Contributions:**

MAW and NSN designed the animal experiments. AS, RCC, AIE, and NSN designed the human experiments. MAW, KS, EET, MMC, and MO performed all animal experiments. MAW, KS, and EET independently verified histological targeting and performed histological immunofluorescent analysis. MAW, ASB, YK, and NSN performed all statistical analyses. MAW and NSN wrote the manuscript, and all authors reviewed and revised the manuscript.

## References:


1. Waschke, L., Kloosterman, N. A., Obleser, J. & Garrett, D. D. Behavior needs neural variability. *Neuron* **109**, 751–766 (2021).
2. Renart, A. & Machens, C. K. Variability in neural activity and behavior. *Current Opinion in Neurobiology* **25**, 211–220 (2014).
3. MacDonald, S. W. S., Karlsson, S., Rieckmann, A., Nyberg, L. & Bäckman, L. Aging-related increases in behavioral variability: relations to losses of dopamine D1 receptors. *J. Neurosci.* **32**, 8186–8191 (2012).
4. Agostino, P. V. & Cheng, R.-K. Contributions of dopaminergic signaling to timing accuracy and precision. *Current Opinion in Behavioral Sciences* **8**, 153–160 (2016).
5. O'Boyle, D. J., Freeman, J. S. & Cody, F. W. The accuracy and precision of timing of self-paced, repetitive movements in subjects with Parkinson's disease. *Brain* **119 ( Pt 1)**, 51–70 (1996).
6. Narayanan, N. S. & Albin, R. L. *Cognition in Parkinson's Disease*. (Elsevier, Acad. Press, 2022).
7. Barkley, R. *ADHD and the Nature of Self-Control*. (The Guilford Press, New York, NY, 1997).
8. Campbell, W. G. Addiction: a disease of volition caused by a cognitive impairment. *Can J Psychiatry* **48**, 669–674 (2003).
9. Buhusi, C. V. & Meck, W. H. What makes us tick? Functional and neural mechanisms of interval timing. *Nat. Rev. Neurosci* **6**, 755–765 (2005).
10. Merchant, H. & de Lafuente, V. Introduction to the neurobiology of interval timing. *Adv. Exp. Med. Biol.* **829**, 1–13 (2014).
11. Merchant, H., Luciana, M., Hooper, C., Majestic, S. & Tuite, P. Interval timing and Parkinson's disease: heterogeneity in temporal performance. *Exp Brain Res* **184**, 233–248 (2008).
12. Singh, A. *et al.* Timing variability and midfrontal ~4 Hz rhythms correlate with cognition in Parkinson's disease. *NPJ Parkinsons Dis* **7**, 14 (2021).
13. Malapani, C., Dubois, B., Rancurel, G. & Gibbon, J. Cerebellar dysfunctions of temporal processing in the seconds range in humans. *Neuroreport* **9**, 3907–3912 (1998).
14. Penney, T. B., Meck, W. H., Roberts, S. A., Gibbon, J. & Erlenmeyer-Kimling, L. Interval-timing deficits in individuals at high risk for schizophrenia. *Brain and cognition* **58**, 109–118 (2005).
15. Ward, R. D. *et al.* Impaired timing precision produced by striatal D2 receptor overexpression is mediated by cognitive and motivational deficits. *Behav. Neurosci.* **123**, 720–730 (2009).
16. Ward, R. D., Kellendonk, C., Kandel, E. R. & Balsam, P. D. Timing as a window on cognition in schizophrenia. *Neuropharmacology* https://doi.org/10.1016/j.neuropharm.2011.04.014 (2011) doi:10.1016/j.neuropharm.2011.04.014.
17. Singh, A. *et al.* Evoked mid-frontal activity predicts cognitive dysfunction in Parkinson's disease. *J Neurol Neurosurg Psychiatry* jnnp-2022-330154 (2023) doi:10.1136/jnnp-2022-330154.
18. Bruce, R. A. *et al.* Experience-related enhancements in striatal temporal encoding. *Eur J Neurosci* **54**, 5063–5074 (2021).
19. Bruce, R. A. *et al.* Complementary cognitive roles for D2-MSNs and D1-MSNs during interval timing. *eLife* **13**, RP96287 (2025).
20. Weber, M. A. *et al.* Glycolysis-enhancing α1-adrenergic antagonists modify cognitive symptoms related to Parkinson's disease. *npj Parkinsons Dis.* **9**, 1–7 (2023).
21. Balci, F. *et al.* Interval timing in genetically modified mice: a simple paradigm. *Genes Brain Behav* **7**, 373–384 (2008).
22. Weber, M. A. *et al.* Amphetamine increases timing variability by degrading prefrontal temporal encoding. *Neuropharmacology* **275**, 110486 (2025).
23. Weber, M. A. *et al.* Alpha-Synuclein Pre-Formed Fibrils Injected into Prefrontal Cortex Primarily Spread to Cortical and Subcortical Structures. *JPD* **14**, 81–94 (2024).
24. Stutt, H. R. *et al.* Sex similarities and dopaminergic differences in interval timing. *Behavioral Neuroscience* **138**, 85–93 (2024).

25. Bova, A. *et al.* Timing, movement, and reward contributions to prefrontal and striatal ramping activity. Preprint at https://doi.org/10.1101/2025.07.02.662841 (2025).
26. Ding, X. *et al.* Diverse activity in prefrontal projections promotes temporal control of action. Preprint at https://doi.org/10.1101/2025.05.12.653607 (2025).
27. Lindgren, H. S., Demirbugen, M., Bergqvist, F., Lane, E. L. & Dunnett, S. B. The effect of additional noradrenergic and serotonergic depletion on a lateralised choice reaction time task in rats with nigral 6-OHDA lesions. *Exp Neurol* **253**, 52–62 (2014).
28. Torres, E. M. & Dunnett, S. B. 6-OHDA Lesion Models of Parkinson's Disease in the Rat. in *Animal Models of Movement Disorders: Volume I* (eds Lane, E. L. & Dunnett, S. B.) 267–279 (Humana Press, Totowa, NJ, 2012). doi:10.1007/978-1-61779-298-4_13.
29. Thiele, S. L., Warre, R. & Nash, J. E. Development of a unilaterally-lesioned 6-OHDA mouse model of Parkinson's disease. *J Vis Exp* 3234 (2012) doi:10.3791/3234.
30. Boyden, E. S., Zhang, F., Bamberg, E., Nagel, G. & Deisseroth, K. Millisecond-timescale, genetically targeted optical control of neural activity. *Nat. Neurosci* **8**, 1263–1268 (2005).
31. Simpson, E. H. *et al.* Lights, fiber, action! A primer on in vivo fiber photometry. *Neuron* **112**, 718–739 (2024).
32. Kim, Y. *et al.* Phase-adaptive brain stimulation of striatal D1 medium spiny neurons in dopamine-depleted mice. *Sci Rep* **12**, 21780 (2022).
33. Kim, Y.-C. *et al.* Optogenetic Stimulation of Frontal D1 Neurons Compensates for Impaired Temporal Control of Action in Dopamine-Depleted Mice. *Curr Biol* **27**, 39–47 (2017).
34. Kim, Y.-C. & Narayanan, N. S. Prefrontal D1 Dopamine-Receptor Neurons and Delta Resonance in Interval Timing. *Cereb Cortex* https://doi.org/10.1093/cercor/bhy083 (2018) doi:10.1093/cercor/bhy083.
35. Larson, T. *et al.* Mice expressing P301S mutant human tau have deficits in interval timing. *Behav Brain Res* **432**, 113967 (2022).
36. Tosun, T., Gur, E. & Balci, F. Mice plan decision strategies based on previously learned time intervals, locations, and probabilities. *Proc Natl Acad Sci U S A* **113**, 787–792 (2016).
37. Weber, M. A. *et al.* Glycolysis-enhancing α1-adrenergic antagonists modify cognitive symptoms related to Parkinson's disease. *npj Parkinsons Dis.* **9**, 32 (2023).
38. Kim, Y.-C. *et al.* Optogenetic Stimulation of Frontal D1 Neurons Compensates for Impaired Temporal Control of Action in Dopamine-Depleted Mice. *Current Biology* **27**, 39–47 (2017).
39. Alberico, S. L., Cassell, M. D. & Narayanan, N. S. The Vulnerable Ventral Tegmental Area in Parkinson's Disease. *Basal Ganglia* **5**, 51–55 (2015).
40. Kim, J., Ghim, J.-W., Lee, J. H. & Jung, M. W. Neural correlates of interval timing in rodent prefrontal cortex. *J. Neurosci.* **33**, 13834–13847 (2013).
41. Xu, M., Zhang, S., Dan, Y. & Poo, M. Representation of interval timing by temporally scalable firing patterns in rat prefrontal cortex. *Proc. Natl. Acad. Sci. U.S.A.* **111**, 480–485 (2014).
42. Kurti, A. N. & Matell, M. S. Nucleus accumbens dopamine modulates response rate but not response timing in an interval timing task. *Behav. Neurosci* **125**, 215–225 (2011).
43. Cohen, J. Y., Haesler, S., Vong, L., Lowell, B. B. & Uchida, N. Neuron-type-specific signals for reward and punishment in the ventral tegmental area. *Nature* **482**, 85–88 (2012).
44. Nestler, E. J. & Carlezon, W. A. The Mesolimbic Dopamine Reward Circuit in Depression. *Biological Psychiatry* **59**, 1151–1159 (2006).
45. Floresco, S. B. & Magyar, O. Mesocortical dopamine modulation of executive functions: beyond working memory. *Psychopharmacology (Berl.)* **188**, 567–585 (2006).
46. Brozoski, T. J., Brown, R. M., Rosvold, H. E. & Goldman, P. S. Cognitive deficit caused by regional depletion of dopamine in prefrontal cortex of rhesus monkey. *Science* **205**, 929–932 (1979).
47. Narayanan, N. S., Land, B. B., Solder, J. E., Deisseroth, K. & DiLeone, R. J. Prefrontal D1 dopamine signaling is required for temporal control. *Proc. Natl. Acad. Sci. U.S.A.* **109**, 20726–20731 (2012).
48. Morales, M. & Margolis, E. B. Ventral tegmental area: cellular heterogeneity, connectivity and behaviour. *Nat Rev Neurosci* **18**, 73–85 (2017).

49. Lammel, S., Ion, D. I., Roeper, J. & Malenka, R. C. Projection-specific modulation of dopamine neuron synapses by aversive and rewarding stimuli. *Neuron* **70**, 855–862 (2011).
50. Root, D. H. *et al.* Distinct Signaling by Ventral Tegmental Area Glutamate, GABA, and Combinatorial Glutamate-GABA Neurons in Motivated Behavior. *Cell Reports* **32**, (2020).
51. Poulin, J.-F. *et al.* Defining Midbrain Dopaminergic Neuron Diversity by Single-Cell Gene Expression Profiling. *Cell Reports* **9**, 930–943 (2014).
52. Ko, J. H. *et al.* Prefrontal dopaminergic receptor abnormalities and executive functions in Parkinson's disease. *Human brain mapping* https://doi.org/10.1002/hbm.22006 (2012) doi:10.1002/hbm.22006.
53. Parker, K. L. *et al.* Delta-frequency stimulation of cerebellar projections can compensate for schizophrenia-related medial frontal dysfunction. *Mol Psychiatry* **22**, 647–655 (2017).
54. Kelley, R. *et al.* A human prefrontal-subthalamic circuit for cognitive control. *Brain* **141**, 205–216 (2018).
55. Parker, K. L., Chen, K.-H., Kingyon, J. R., Cavanagh, J. F. & Narayanan, N. S. Medial frontal ~4-Hz activity in humans and rodents is attenuated in PD patients and in rodents with cortical dopamine depletion. *Journal of Neurophysiology* **114**, 1310–1320 (2015).
56. Narayanan, N. S., Jourahmad, Z., Cole, R. C. & Cavanagh, J. F. Cognition falters at ~4 Hz in Parkinson's disease. *Trends Cogn Sci* **28**, 789–791 (2024).
57. Salehi, N. *et al.* Theta frequency deep brain stimulation in the subthalamic nucleus improves working memory in Parkinson's disease. *Brain* awad433 (2024) doi:10.1093/brain/awad433.
58. Scangos, K. W., Carter, C. S., Gurkoff, G., Zhang, L. & Shahlaie, K. A pilot study of subthalamic theta frequency deep brain stimulation for cognitive dysfunction in Parkinson's disease. *Brain Stimul* **11**, 456–458 (2018).
59. Cole, R. C. *et al.* Theta-frequency subthalamic nucleus stimulation increases decision threshold. *Brain Stimul* S1935-861X(25)00209–8 (2025) doi:10.1016/j.brs.2025.05.105.